nature chemistry

ARTICLES

PUBLISHED ONLINE: 23 OCTOBER 2011 | DOI: 10.1038/NCHEM.1174

Cytocompatible click-based hydrogels with dynamically tunable properties through orthogonal photoconjugation and photocleavage reactions

Cole A. DeForest[1] and Kristi S. Anseth[1,2]*

To provide insight into how cells receive information from their external surroundings, synthetic hydrogels have emerged as systems for assaying cell function in well-defined microenvironments where single cues can be introduced and subsequent effects individually elucidated. However, as answers to more complex biological questions continue to be sought, advanced material systems are needed that allow dynamic alteration of the three-dimensional cellular environment with orthogonal reactions that enable multiple levels of control of biochemical and biomechanical signals. Here, we seek to synthesize one such three-dimensional culture system using cytocompatible and wavelength-specific photochemical reactions to create hydrogels that allow orthogonal and dynamic control of material properties through independent spatiotemporally regulated photocleavage of crosslinks and photoconjugation of pendant functionalities. The results demonstrate the versatile nature of the chemistry to create programmable niches to study and direct cell function by modifying the local hydrogel environment.

Since its conception by Sharpless in 2001[1], the concept of click chemistry has been rapidly adopted by many disciplines, perhaps most notably in materials science, with annual publication numbers continuing to increase exponentially[2–5]. The click philosophy idealizes reactions that enable researchers to covalently link two reactants in a straightforward, modular and high-yielding manner. The copper(I)-catalysed azide-alkyne cycloaddition (CuAAC) is frequently billed as the quintessential example in meeting these criteria. Although each click reaction has a number of desirable properties, their true benefit lies in the orthogonality of these reactions with respect to many common reactive groups (for example, amines, alcohols and acids)[6]. Reaction orthogonality enables independent control over multiple functional groups in a single system, opening the door to the synthesis of materials with ever-increasing complexity for an ever-expanding list of applications.

There is also a growing interest in chemical reactions that can be performed in the presence of live cells[6]. These reactions must proceed mildly in an aqueous medium and defined chemical environment (5% CO_2 and atmospheric O_2 levels), under regulated pH (7.4), temperature (37 °C) and osmolarity (~300 mOs M), and involve non-toxic reactive moieties and (by)products. The requirement that reactions proceed under physiological conditions is a stringent constraint and presents severe limitations on reaction selection. In particular, there are few chemistries that proceed in a specific manner while limiting side reactions with the plethora of functional groups that are found in biological systems. These elite reactions are considered bio-orthogonal and are necessary for chemically probing and directing biological function.

In many instances, an ideal cytocompatible reaction would not only be selected by its bio-orthogonality, but also by its capacity to be controlled in both time and space. Accordingly, photochemical reactions are widely regarded for their spatiotemporal control, where the reaction of interest is defined by when and where light is delivered to the system[7]. Photolithographic techniques, where masked light is projected directly onto a sample, enable photoreactions to be confined to specific regions within a sample as defined by a two-dimensional mask pattern, while focused laser light (either single- or multiphoton) provides full three-dimensional control over where a specific reaction occurs within the volume of a material. Although the effects of attenuation and scattering must be carefully taken into consideration, light-based chemistries have become a powerful tool for materials synthesis and spatial modification, owing to their ease of implementation and the fact that inexpensive light sources are readily available, and have become indispensible in the formation and subsequent modification of biomaterials.

So far, biocompatible light-based chemistries have enabled control in space and time of either the gel degradation or gel chemistry of synthetic cell culture systems. By introducing chemical functionalities in user-defined patterns within the material, cell spreading and migration have been explicitly controlled in three dimensions[8–13]. Also, cell outgrowth and stem cell fate have been directed by altering the structural properties of the gel[14–18]. Independent control over both the physical and chemical make-up of the material in three dimensions, as well as in time, would allow dynamic tailoring of the microenvironment of a cell, but as yet this has not been demonstrated. Such four-dimensional control of material properties would be tremendously advantageous in a number of biomaterial applications, including three-dimensional cell culture, stem cell expansion, cancer metastasis and tissue regeneration. Of further importance and novelty, the ability for the experimenter to control gel properties at any point in space and time enables opportunities for unique experiments, such as the ability to dynamically introduce a cell ligand or allow cell–cell interactions at specified locations. These programmable cell culture niches would facilitate the ability to perform newfound experiments and answer questions about the dynamic exchange of information between a cell and its niche. In this Article, we present one such system where multiple wavelengths of light are

[1]Department of Chemical and Biological Engineering, University of Colorado, UCB Box 424, Boulder, Colorado 80309-0424, USA, [2]Howard Hughes Medical Institute, University of Colorado, UCB Box 424, Boulder, Colorado 80309-0424, USA. *e-mail: kristi.anseth@colorado.edu

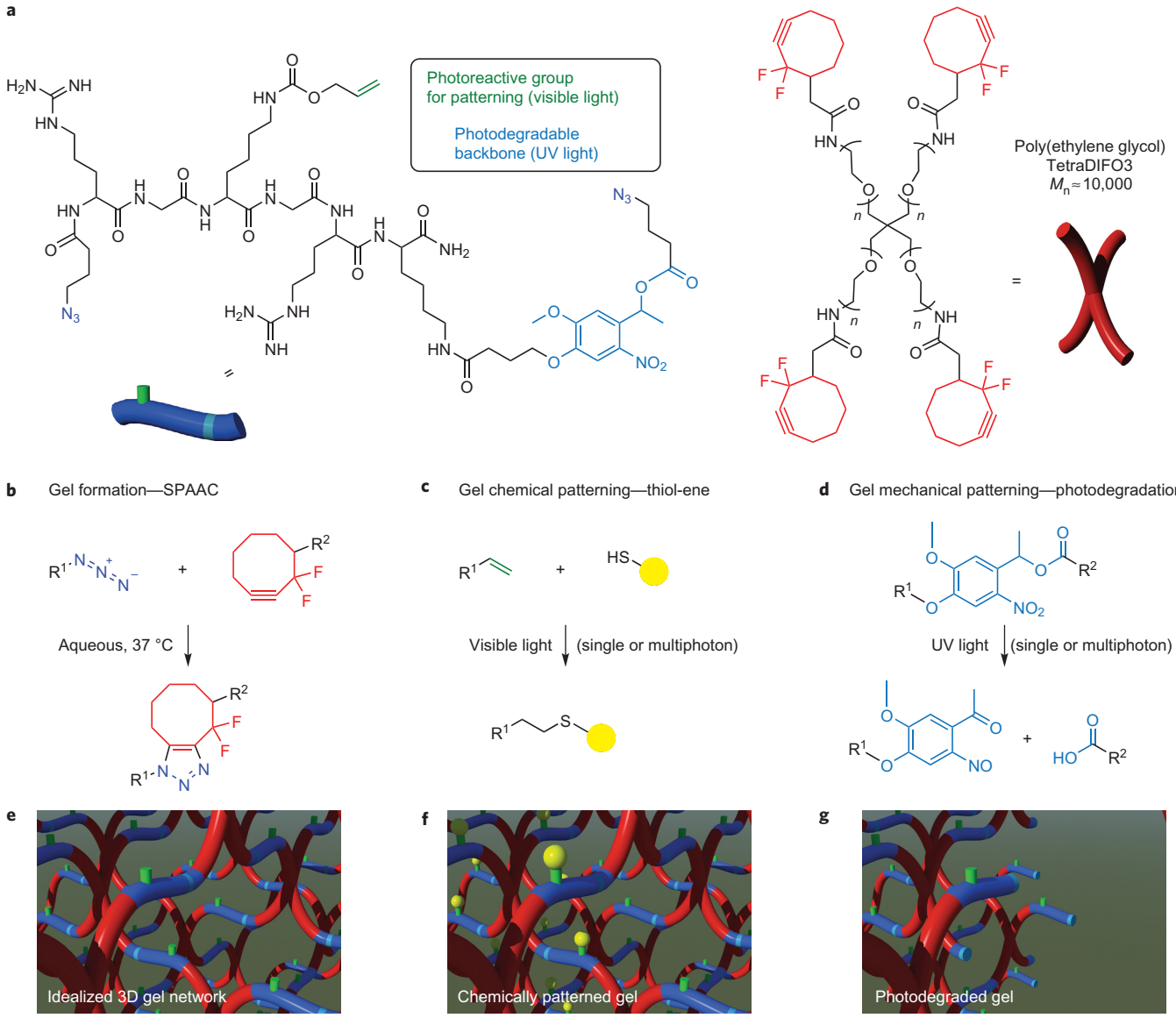

Figure 1 | Synthesis, photocoupling and photodegradation for tuning chemical and physical properties of click-based hydrogels. a,**b**, Click-functionalized macromolecular precursors (PEG-tetraDIFO3 and bis(azide)-functionalized polypeptides) form a three-dimensional ideal hydrogel structure (**a**) by means of a step-growth polymerization mechanism via the SPAAC reaction (**b**). **c**, In the presence of visible light ($\lambda = 490$–650 nm or 860 nm), thiol-containing biomolecules are covalently affixed to pendant vinyl functionalities throughout the hydrogel network via the thiol-ene reaction. **d**, A nitrobenzyl ether moiety within the backbone of the polymer network undergoes photocleavage in the presence of single or multiphoton ultraviolet light ($\lambda = 365$ nm or 740 nm) that results in photodegradation of the network. **e**–**g**, Schematics of the formed SPAAC-based idealized gel (**e**), the network after thiol-ene functionalization (**f**) and the material after photodegradation (**g**).

used to independently control the functionality and architecture of a hydrogel network formed by means of a copper-free alkyne-azide reaction (Fig. 1). Each of the reactions is cytocompatible, and both photoconjugation and photocleavage reactions are used to spatiotemporally regulate material properties, including the presentation of integrin-binding motifs and network erosion through cleavage of crosslinking moieties. This platform allows gel parameters to be tuned in real time, and the results demonstrate how spatiotemporal regulation of material properties can be used to direct the function of embedded cells.

Results and discussion

A four-arm poly(ethylene glycol) (PEG) tetracyclooctyne ($M_n \approx$ 10,000 Da) was reacted with a bis(azide) di-functionalized polypeptide (Azide–RGK(alloc)GRK(PLazide)–NH_2) via a copper-free, strain-promoted azide-alkyne cycloaddition (SPAAC) reaction between terminal difluorinated cyclooctyne (DIFO3) and azide ($-N_3$) moieties with 1:1 stoichiometry at 10 wt% total macromer concentration to form an idealized three-dimensional network with minimal local defects. The ring strain and electronegative fluorine substituents of DIFO3 enable the SPAAC reaction to proceed rapidly, without a catalyst, and in the presence of cells[19]. Network gelation occurs ~2 min after mixing, as estimated by the crossover point of the rheological storage (G') and loss (G'') moduli (Supplementary Fig. S1). By including a synthetic polypeptide in the gel formulation, the precise chemical make-up of the material is tailored readily by choice of the amino-acid sequence, allowing one to tailor the biofunctionality (for example, enzymatic degradability, integrin-binding ligands, protein affinity binding sites) and introduce bio-orthogonal reactive moieties (for example, vinyl

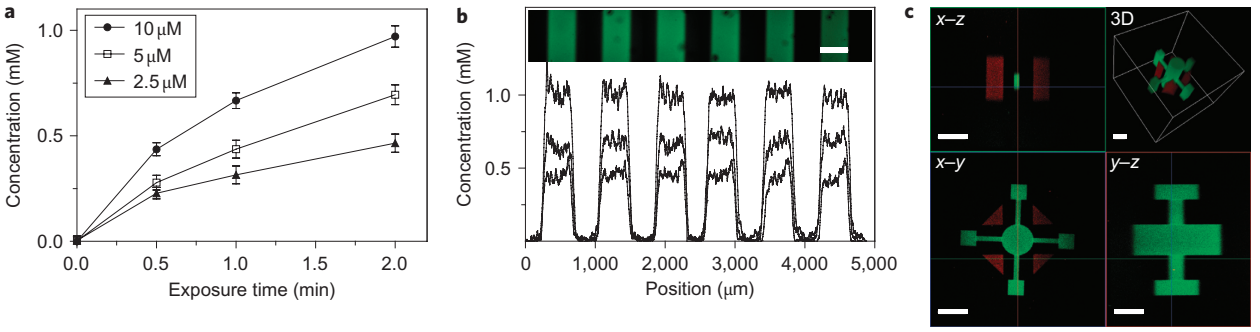

Figure 2 | Biochemical patterning within preformed click hydrogels using visible light. Upon swelling thiol-containing biomolecules into pre-formed gels, pendant functionalities are affixed to the hydrogel backbone via the thiol-ene reaction on exposure to visible light ($\lambda = 490$–650 nm). **a**, The final patterned concentration of a fluorescent RGD peptide (AF_{488}-AhxRGDSC-NH_2) depends on the amount of photoinitiator present (2.5, 5 and 10 μM eosin Y), as well as the exposure time to visible light (0–2 min, 10 mW cm^{-2}). Error bars represent the standard deviation of experiments performed in triplicate. **b**, Network functionalization with pendant fluorescently labelled peptides is confined to user-defined regions within pre-formed gels using photolithography (0.5, 1 or 2 min exposure with increased patterning concentration for increased exposure time, 10 mW cm^{-2}, 10 μM eosin Y). **c**, The photocoupling reaction is controlled in three dimensions by rastering the focal point of multiphoton laser light ($\lambda = 860$ nm) over defined volumes within the gel, affording micrometre-scale resolution in all spatial dimensions. The patterning process can be repeated many times to introduce multiple biochemical cues within the same network, as demonstrated by the red- and green-labelled patterned peptides within the same gel. Images represent confocal projections and three-dimensional renderings. Scale bars, 400 μm (**b**) and 100 μm (**c**).

groups, azides). Ultimately, the timescale and mechanism of the SPAAC reaction permits high viability (>95%) during encapsulation of both established cell lines, as well as primary cell types (Supplementary Fig. S11)[8].

Biochemical control via thiol-ene photoconjugation. Incorporated into the synthetic peptide is the commercially available lysine(allyloxycarbonyl) (alloc) amino acid, in which the alloc protecting group is stable to standard solid-phase peptide synthesis methods and contains a vinyl functionality that is readily photocoupled to thiol-containing compounds, such as cysteine, via the thiol-ene reaction. Although a number of reactions can be controlled with light, including the CuAAC by a photogenerated copper(I) catalyst[20], the radical-mediated thiol-ene addition has emerged as a versatile click reaction that can be photochemically initiated[21,22]. This reaction, which involves the catalytic propagation of a thiyl radical across an olefin (−C=C), and subsequent chain transfer from the resulting carbon radical to a thiol (−SH), has gained recent interest as an approach to functionalize systems with biomolecules[8,23,24], control dendrimer formation[25], as well as synthesize other complex materials[26,27]. The propagating thiyl radical is readily generated in the presence of both cleavage type, as well as hydrogen-abstracting photoinitiators[28], enabling thiol-containing molecules to be physically linked to vinyl-functionalized moieties over a variety of light conditions including in the visible range. This reaction can be used with peptides, thiolated full proteins, and small molecules that are individually capable of diffusing throughout the hydrogel (Supplementary Figs S2, S3), although peptides that contain free thiols in their bioactive domain may exhibit reduced biological effect upon thiol-ene coupling. The reaction is regarded as cytocompatible (Supplementary Fig. S11), as well as bio-orthogonal, facilitating its use in biological systems[21], and enables materials to be functionalized dynamically with specific molecules of interest at any given location and time.

After gel formation, fluorescently labelled thiol-containing biomolecules were swollen into the network together with a small amount of eosin Y photoinitiator (2.5–10 μM), which was followed by visible light irradiation ($\lambda = 490$–650 nm) at low intensities (10 mW cm^{-2}) and short durations (0.5–2 min). The extent of photocoupling was visualized and quantified using confocal microscopy and was controlled by photoinitiator concentration and exposure time (Fig. 2a). Specifically, patterning concentrations between 0 and 1 mM were obtained with short light exposures of only a few minutes. By irradiating through a photomask, patterning was confined to specific locations throughout the gel, as demonstrated by the transfer of a 400-μm-wide line pattern through the depth of the sample (Fig. 2b, Supplementary Fig. S4). Multiphoton initiation techniques ($\lambda = 860$ nm) were also used to create elaborate, user-defined, three-dimensional biochemical patterns within the hydrogel (Fig. 2c). Here, a 300 × 400 × 400 μm interconnected three-dimensional structure composed of multiple shapes and two distinct peptides was created. The resolution that we achieve with multiphoton-based patterning is ~1 μm in the *x*–*y* plane and ~3–5 μm in the *z* plane, values that are typical of multiphoton imaging methods and represent a limitation of the optics and not the chemistry. The photocoupling process can be repeated many times over, with each cycle requiring a timescale of a few hours for introduction and removal of the signal via diffusion (depending on the gel dimensions). Thus, multiple signals can be incorporated with micrometre-scale patterning resolution on time and size scales that are relevant for many cell culture experiments.

Biophysical control via photodegradation. The utility of a peptide linker enables desired sequences, as well as desired functionalities, to be precisely incorporated in a modular fashion. In addition to the pendant alloc vinyl functionality, the peptide includes a photodegradable nitrobenzyl ether moiety (PLazide) within its backbone, enabling photocleavage of the crosslinks upon exposure to ultraviolet light (either $\lambda = 365$ nm for single-photon or $\lambda = 740$ nm for multiphoton[14,29]). Specifically, the irreversible photocleavage of an *o*-nitrobenzyl ether moiety into nitroso- and acid-terminated by-products permits a previously intact chemical linkage to be cleaved photolytically. The photolabile group degrades under cytocompatible irradiation conditions, including 365 nm light[29], and has been used for the uncaging of proteins[30], to cleave peptides from a solid support[31], as well as to control cell adhesion[9,32]. Functionality has also been incorporated into materials to produce networks that are capable of degrading in the presence of light[14,33,34], allowing the effects of physical material cues on cell function to be probed[35–37].

Based on kinetic nuclear magnetic resonance (NMR) as well as photorheometry studies, the photoscission of the PLazide moiety

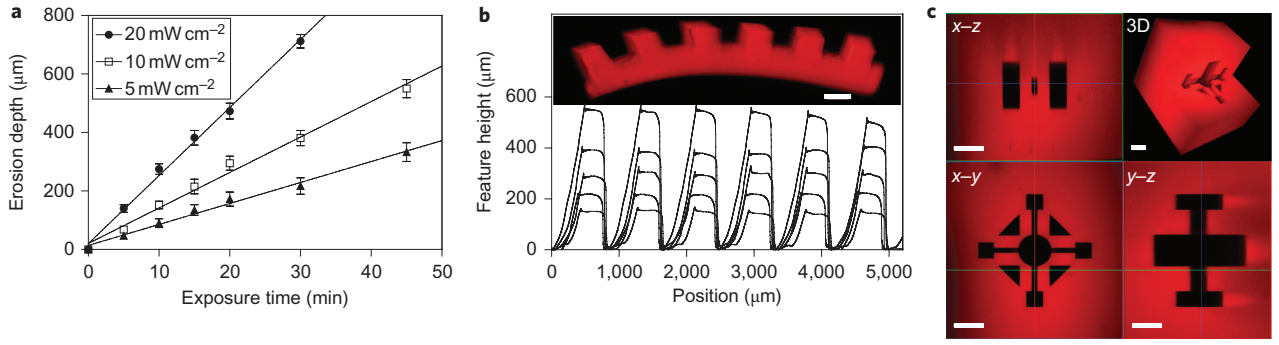

Figure 3 | Biophysical patterning within pre-formed click hydrogels using ultraviolet light. In the presence of ultraviolet light ($\lambda = 365$ nm), photolabile functionalities within the hydrogel crosslinks undergo an irreversible cleavage, thereby decreasing total network connectivity, resulting in local material degradation and removal of the fluorescent hydrogel material. **a**, In optically thick samples, the depth of photodegradation is directly related to the incident light intensity (5, 10 and 20 mW cm^{-2}), as well as the exposure time to visible light (0–45 min). Error bars represent the standard deviation of experiments performed in triplicate. **b**, Using mask-based photolithographic techniques, network degradation was confined to user-defined regions within fluorescently labelled gels (10, 15, 20, 30 and 45 min, feature height increasing with exposure time), as measured by profilometry. **c**, The photodegradation reaction is controlled in three dimensions with micrometre-scale resolution in all dimensions using focused multiphoton laser light ($\lambda = 740$ nm). Images represent confocal projections and three-dimensional renderings. Scale bars, 400 μm (**b**) and 100 μm (**c**).

(Supplementary Fig. S5) was found to follow a first-order degradation with a rate constant k that can be expressed as

$$k = \frac{\varphi \varepsilon I}{N_A h \nu}$$

where φ is the quantum yield (determined to be 0.020), ε is the molar absorptivity of the sample (4,780 M^{-1} cm^{-1} for PLazide at $\lambda = 365$ nm), I is the intensity of light, N_A is Avogadro's number, h is Planck's constant, and ν is the frequency of the associated electromagnetic wave (Supplementary Figs S6, S7, S8). For typical exposure conditions ($\lambda = 365$ nm, 10 mW cm^{-2}), k was determined to be 2.9×10^{-3} s^{-1}, and correlates well with other photodegradable moieties[14,31]. Physical channels were eroded downward from the surface of optically thick samples, with the depth of photodegradation directly related to the total light intensity (5, 10 and 20 mW cm^{-2}), as well as the exposure time of ultraviolet light (0–45 min) (Fig. 3a, Supplementary Fig. S9) and the total light dosage delivered to the material (Supplementary Fig. S10). As with the photocoupling reaction, the photocleavage reaction was confined to regions of interest within the sample using photolithographic processes to create channels of varying depths (~150–600 μm) (Fig. 3b), as well as multiphoton patterning approaches to erode precisely defined three-dimensional regions of interest with user-defined shapes and connectivity (Fig. 3c, $\lambda = 740$ nm). Each process affords a high level of patterning fidelity, similar to that obtained by the photocoupling reaction.

Orthogonal photoreactions for advanced three-dimensional cell culture. The utility of the photocoupling and photocleavage reactions ultimately stems from their ability to be performed orthogonally, such that both network mechanical and chemical make-up are controlled independently. The peak values of absorbance for the photolabile group and the visible photoinitiator were found to be ~350 and ~520 nm, respectively, with relatively little overlap of the absorbance spectra (Fig. 4a). As eosin Y also has a low absorbance at $\lambda = 365$ nm, photocoupling during photodegradation was readily prevented by performing degradation only in the absence of a photoinitiator. Alternatively, photocoupling was initiated first with visible light ($\lambda = 490$–650 nm) and photodegradation was commenced with subsequent ultraviolet irradiation. The orthogonality of these reactions was confirmed by solution NMR studies where photocleavage was quantified under both visible and ultraviolet light initiation conditions using model compounds (Fig. 4b). To illustrate the orthogonality of the reactions within the same material system, a buffalo logo was first photocoupled within the three-dimensional network using visible light, and user-defined letters (CU) were eroded within the fluorescent logo at a later time (Fig. 4c). Photodegradation was confirmed to be confined only to the areas of interest by bright-field microscopy (Fig. 4d), as well as with the disappearance of the fluorescently labelled reporter peptide, indicating that cues can be spatially coupled and subsequently removed with orthogonal reactions.

To provide a demonstration of the potential utility of these two photoreactions for advanced three-dimensional cell culture, Fig. 5 presents an approach where one might assay the specific effects of a variety of biomolecular cues on cell function within an otherwise uniform gel culture platform. Here, human mesenchymal stem cells (hMSCs) were encapsulated in gels synthesized by means of SPAAC chemistry, and their cellular microenvironment was patterned using the thiol-ene photocoupling reaction with perpendicular lines (width = 200 μm) of integrin-binding peptide ligands, RGD and PHSRN (~1 mM each). These peptide sequences are both derived from sequences found in fibronectin and are known to elicit some degree of synergy on cell adhesion[38]. The patterning created a repeating array of four distinct biochemical culture conditions (no cue, RGD alone, PHSRN alone, or both RGD and PHSRN) within the same gel (Fig. 5a). At a later time point, the photodegradation reaction was exploited to capture cells in spatially defined regions of interest by exposing the gel to a given condition of light to induce erosion and liberate cells from their three-dimensional culture environment (Fig. 5b). This process can be repeated many times at different time points and locations to collect cells that have been exposed to either the same or different biochemical conditions, demonstrating full spatiotemporal control over cell subpopulation sampling (Fig. 5c). The released cells are readily collected, subsequently plated, expanded and made available for additional biological assays, including those that may be more difficult to perform on encapsulated cells. hMSCs remained viable (>95%) throughout the entire process (Supplementary Fig. S11). We plated the released hMSCs and visualized their cytoskeletal organization using a fluorescent phalloidin, which stains for F-actin (Fig. 5d).

To further demonstrate how these reactions can be used to manipulate cellular functions in a spatiotemporally regulated manner, a cell-laden (3T3 fibroblasts) fibrin clot was encapsulated

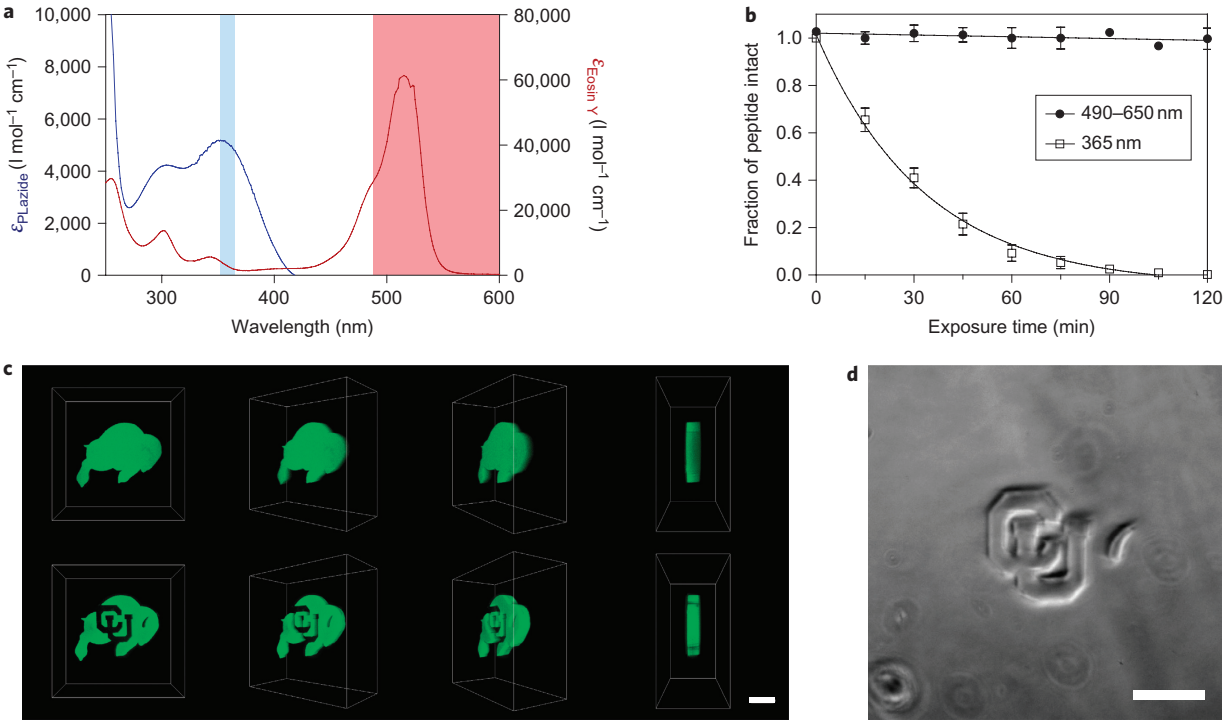

Figure 4 | Orthogonality of photocoupling and photodegradation reactions. a, Peak absorbances for the photoinitiator (red) and the photolabile group (blue) are well separated (~520 and ~350 nm, respectively), thus enabling photocoupling and photodegradation reactions to be performed independently from one another using different light sources (illustrated with coloured bars). **b**, NMR studies indicate that the photodegradable moiety cleaves readily in the presence of ultraviolet light ($\lambda = 365$ nm, 10 mW cm^{-2}), but remains intact when exposed to the visible light used to initiate the photocoupling reaction ($\lambda = 490$–650 nm, 10 mW cm^{-2}). Error bars represent the standard deviation of experiments performed in triplicate. **c**, Multiphoton visible light was first used to couple a fluorescently labelled peptide within the centre of the hydrogel in a user-defined three-dimensional pattern (top, buffalo), and the network was subsequently degraded locally with multiphoton ultraviolet light, thereby removing the peptide from selected regions (bottom, CU and horn). **d**, Bright-field microscopy confirms that photocleavage is confined only to user-defined locations within the gel, and that the photocoupling light conditions do not give rise to undesired degradation. Images in **c** represent three-dimensional renderings of confocal *z*-stacks. Scale bars, 100 μm.

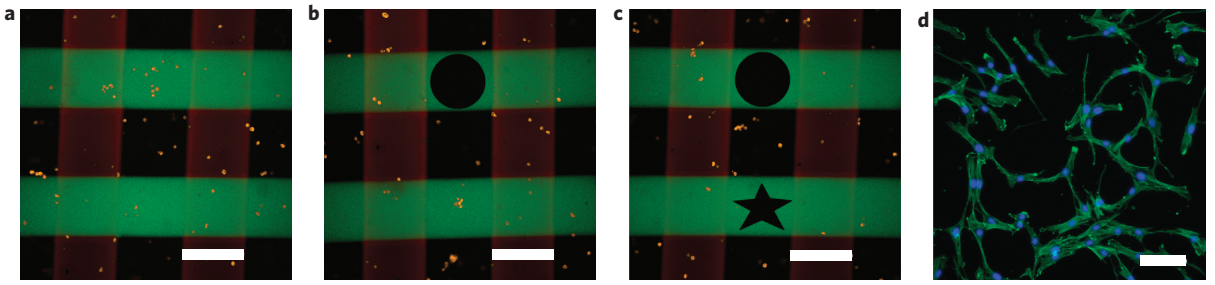

Figure 5 | Culture and recovery of hMSCs from hydrogel microenvironments. CellTracker Orange-labelled hMSCs were encapsulated within the click hydrogel formulation at 5×10^6 cells/ml. **a**, At 24 h post-encapsulation, perpendicular 200-μm-wide lines of ~1 mM RGD and PHSRN were patterned throughout the hydrogel via thiol-ene photocoupling to create an array of four distinct biochemical conditions (no cue, RGD, PHSRN, RGD and PHSRN). **b**, Four hours later, channels of user-defined shape (cylindrical) were eroded down from the surface of the hydrogel to capture entrapped cells exposed to a specific cue. **c**, This process was repeated 1 h later to release entrapped cells within a different location of the material and a different shape (star-shaped cylinder). **d**, The released cells were isolated by centrifugation, cultured in a 96-well plate for 48 h, and their cytoskeletons visualized with fluorescent phalloidin. In **a**–**c**, RGD is shown in green, PHSRN in red and hMSCs in orange. Images represent single confocal slices within the three-dimensional gel. In **d**, F-actin is shown in green and nuclei in blue. Image represents inverted fluorescence micrograph. Scale bars, 200 μm (**a**–**c**), 50 μm (**d**).

within the click hydrogel formulation. After 2 h, physical channels were eroded radially from the spherical clot by multiphoton photodegradation of the network to direct collective cell migration. Only specific regions of the gel were functionalized with RGD via the thiol-ene photocoupling reaction. Cells were found to leave the clot and migrate into the patterned hydrogel channels, but only when eroded migration channels were present and their surfaces decorated with the RGD adhesive ligand (Fig. 6a). Using two-photon patterning techniques, cell outgrowth was explicitly directed in all three spatial dimensions (Fig. 6b). This directed outgrowth can be performed in the presence of other encapsulated cells or with combinations of cell types. For example, hMSCs were encapsulated in the gel surrounding the 3T3-fibroblast-laden clot, and the fibroblasts were directed into the surrounding hMSC microenvironment in a manner controlled by changes in the local gel environment. The patterned 3T3 fibroblasts were found to create complex structures in

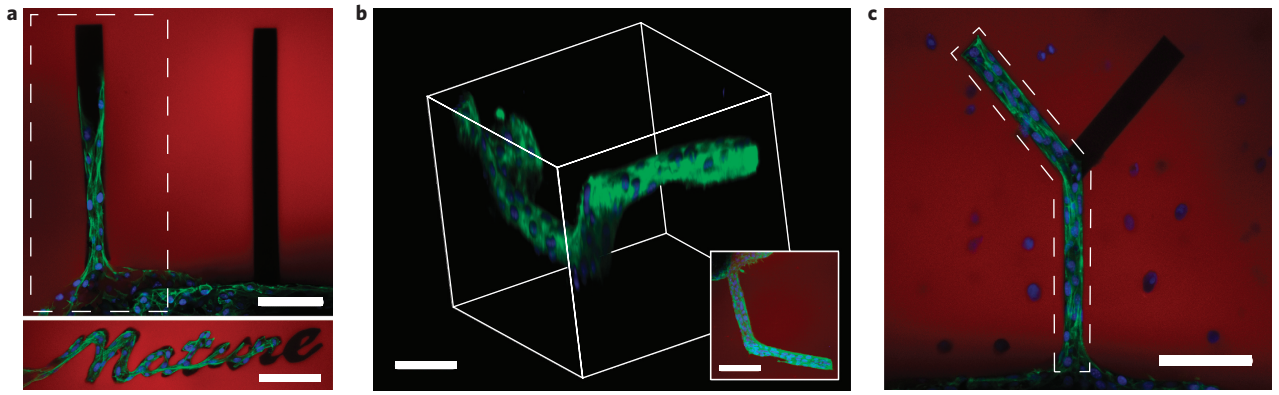

Figure 6 | Directed three-dimensional cell motility within patterned hydrogels. a, A fibrin clot containing 3T3 fibroblasts was encapsulated within the click hydrogel formulation. Chemical channels of RGD, a cell-adhesive fibronectin motif, as well as physical channels of user-defined shape were created radially out of the roughly spherical clot. The combination of having physical space to spread into as well as chemical moieties to bind to was required for collective cell migration. By day 10, cells were found to migrate only down the physical channel functionalized with RGD. **b**, By creating three-dimensional functionalized channels, cell outgrowth was controlled in all three spatial dimensions, with the image inset illustrating a top-down projection. **c**, Outgrowth of 3T3 fibroblast cells was controlled in the presence of encapsulated hMSCs and confined to branched photodegraded channels functionalized with RGD. The regions of RGD functionalization are depicted by the dashed polygons in **a** and **c**. Hydrogel is shown in red, F-actin in green and cell nuclei in blue. Scale bars, 100 μm.

the presence of encapsulated hMSCs (Fig. 6c). These photoreactions are included to demonstrate how one might engineer complex, multicellular structures, ultimately expanding the potential for engineering tissue constructs with spatially varying cellularity in advanced bioreactors or culture systems.

As presented, this work makes use of two novel photoreaction schemes to combine and exploit features of previously mutually exclusive technologies. Namely, the physical and chemical properties of the network can be controlled independently with orthogonal light-based chemistries, allowing for real-time manipulation of cell function within a simplified synthetic microenvironment. These reactions are performed dynamically with full spatiotemporal control, enabling full user direction over these programmable cell niches. The cytocompatibility of the reaction processes should enable newfound opportunities for experiments to test basic hypotheses about critical events regulating cell–materials interactions at multiple time and size scales and, with this knowledge, improve strategies for stem cell culture, biomaterial design, three-dimensional cell culture assays and tissue regeneration.

Methods

Synthesis of click-functionalized macromolecular precursors. For the synthesis of PEG-tetraDIFO3, DIFO3[19,39] (121 mg, 0.6 mmol; Supplementary Fig. S12) and 2-(1H-7-azabenzotriazol-1-yl)–1,1,3,3-tetramethyl uronium hexafluorophosphate methanaminium (HATU, 225 mg, 0.6 mmol, Anaspec) were dissolved in minimal dimethylformamide (DMF, 5 ml) with *N*,*N*-diisopropylethylamine (DIEA, 210 μl, 1.2 mmol) and reacted for 5 min at room temperature. This solution was then added to four-arm PEG tetraamine ($M_n \approx 10{,}000$ Da, 1 g, 0.4 mmol NH_2, JenKem) and stirred overnight, concentrated, dissolved in dH_2O, dialysed (molecular weight cutoff, MWCO ≈ 2 kDa, SpectraPor), filtered and lyophilized to yield a white powder (1.03 g, 96%). Functionalization was confirmed to be >95% by ^{1}H-NMR.

For the synthesis of bis(azide)-functionalized photodegradable peptide crosslinker, the allyl-ester containing peptide H-RGK(alloc)GRK(dde)-NH_2 was synthesized (Protein Technologies Tribute peptide synthesizer) through Fmoc solid-phase methodology and HATU activation. 4-Azidobutanoic acid (Supplementary Fig. S13) was coupled to the N-terminal amine with HATU, the 1-(4,4-dimethyl-2,6-dioxacyclohexylidene)ethyl (Dde) group was removed with 2% hydrazine monohydrate (Sigma) in DMF (3 × 10 min), and 4-(4-(1-(4-azidobutanoyloxy)ethyl)-2-methoxy-5-nitrophenoxy)butanoic acid (PLazide; Supplementary Fig. S13) was coupled to the ε-amino group of the C-terminal lysine. Resin was treated with trifluoroacetic acid/triisopropylsilane/water (95:2.5:2.5) for 2 h and precipitated in and washed (2×) with ice-cold diethyl ether. The crude peptide was purified using semi-preparative reversed-phase high-performance liquid chromatography (RP-HPLC) (Waters Delta Prep 4000) using a 70 min linear gradient (5–95% of acetonitrile and 0.1% trifluoroacetic acid) and lyophilized to give the product (Azide–RGK(alloc)GRK(PLazide)–NH_2) as a fluffy, yellow solid. Peptide purity was confirmed with analytical RP-HPLC and matrix-assisted laser desorption–ionization time-of-flight mass spectrometry (Applied Biosystems DE Voyage) using a-cyano-4-hydroxycinnamic acid matrix (Sigma): calculated ($[M + H]^+$ 1,288.4); observed ($[M + H]^+$ 1,288.1) (Supplementary Fig. S14).

For the synthesis of fluorescently labelled adhesive ligand, H–AhxRGDSC–NH_2 (0.5 mmol) was synthesized and modified with Alexa Fluor 488 carboxylic acid, 2,3,5,6-tetrafluorophenyl ester (2 mg, Invitrogen) in DMF overnight at room temperature. The peptide was cleaved from resin, precipitated and lyophilized to give a yellow solid (denoted AF_{488}–AhxRGDSC–NH_2). AF_{633}–AhxPHSRNC–NH_2 was synthesized in a similar manner.

Gel formation. Hydrogels were created by mixing 10 wt% total macromer photodegradable, photocouplable click gel formulation in media between azide-functionalized (Supplementary Fig. S15) and Rain-X-treated glass slides spaced at a known distance (typically 500 μm), and reacted for 30 min at 37 °C. The slides were separated, and the gel remained covalently attached to the azide-functionalized slide.

Biochemical patterning. Hydrogels were swollen in phenol red-free media containing 3 mg ml^{-1} patterning agent AF_{488}–AhxRGDSC–NH_2 and eosin Y (10 μM) for 1 h. For photolithographic-based experiments, gels were exposed to collimated visible light (λ = 490–650 nm), achieved with an Acticure (EXFO) high-pressure mercury lamp equipped with an internal band-pass filter (350–650 nm) and an external 490 nm long-pass filter (Edmund Optics), through a patterned chrome photomask. Alternatively, three-dimensional patterning was obtained using two-photon techniques where subvolumes within the hydrogel were selectively exposed to pulsed laser light (λ = 860 nm, power = 350 mW μm^{-2}, scan speed = 1.27 μs μm^{-2}) at 1 μm *z*-plane increments on a 710 LSM NLO confocal microscope stage (Carl Zeiss) equipped with a ×20/0.8 Plan-Apochromat objective (NA = 1.0). Unreacted patterning agent and initiator were swollen into fresh media as the sample was gently agitated on an orbital shaker (2 h), yielding the final patterned hydrogel. In both the photolithographic and multiphoton patterning techniques, photocoupling of the peptide was confined to volumes exposed to light within the material and was visualized by fluorescent confocal microscopy.

Biophysical patterning. Gels containing 0.125 mM Alexa Fluor 594 azide (Invitrogen) were patterned using photolithographic techniques, where hydrogels were exposed to collimated ultraviolet light (λ = 365 nm) from an Omnicure S1000 (EXFO) high-pressure mercury lamp equipped with an internal band-pass filter (365 nm). Three-dimensional patterning was obtained using two-photon techniques where regions of interest (*x*–*y* control) within the hydrogel were selectively exposed to pulsed laser light (λ = 740 nm, power = 670 mW μm^{-2}, scan speed = 1.27 μs μm^{-2}). Photodegraded monomer was swollen into fresh media, yielding the final patterned hydrogel.

Cell culture. NIH 3T3s (mouse) were cultured in high-glucose Dulbecco's modified Eagle's medium (DMEM, Gibco) containing 10% fetal bovine serum (Invitrogen), 1% penicillin/streptomycin (Gibco), 0.2% fungizone and 0.4% gentamicin. hMSCs were cultured in low-glucose DMEM with 10% fetal bovine serum, 1% penicillin/streptomycin, 0.2% fungizone and 0.4% gentamicin. All cells were maintained in 5% CO_2 at 37 °C. Cells were used between passages P4 and P6.

Fibrin clot encapsulation. Cells were suspended at 10 × 10^6 cells/ml in a fibrinogen solution (10 mg ml^{-1} in PBS, Sigma) containing thrombin (5 U ml^{-1}, Sigma) and reacted for 30 min at 37 °C. The formed cell-laden clots were suspended in a 10 wt%

total macromer photodegradable, photocouplable click gel formulation sandwiched between azide-functionalized (Supplementary Fig. S10) and Rain-X-treated glass slides spaced at 1 mm, and reacted for an additional 30 min at 37 °C. The slides were separated, and the gel remained covalently attached to the azide-functionalized slide. After 2 h in media, physical channels were patterned into the network with two-photon patterning ($\lambda = 740$ nm). The media was then supplemented with Ac–RGDSC–NH_2 (3 mg ml^{-1}) and eosin Y (10 μM), equilibrated for 1 h, and selected regions within the gel were biochemically decorated with RGD ($\lambda = 860$ nm). On day 10, the hydrogels were fixed in formalin for 1.5 h, followed by cell permeabilization with 0.5% Triton X-100 (Fisher) in PBS for 2 h. The samples were blocked with 3% bovine serum albumin (BSA, Sigma) in PBS for 1 h and rinsed with PBS. F-actin was visualized using Alexa Fluor 488 Phalloidin Conjugate (5 U ml^{-1}, Invitrogen), and nuclei were stained with DAPI (500 nM, Invitrogen), each for 2 h. The samples were washed with PBS before confocal visualization.

Received 21 June 2011; accepted 13 September 2011; published online 23 October 2011

References

1. Kolb, H. C., Finn, M. G. & Sharpless, K. B. Click chemistry: diverse chemical function from a few good reactions. *Angew. Chem. Int. Ed.* **40,** 2004–2021 (2001).
2. Kolb, H. C. & Sharpless, K. B. The growing impact of click chemistry on drug discovery. *Drug Discov. Today* **8,** 1128–1137 (2003).
3. Moses, J. E. & Moorhouse, A. D. The growing applications of click chemistry. *Chem. Soc. Rev.* **36,** 1249–1262 (2007).
4. Hawker, C. J. & Wooley, K. L. The convergence of synthetic organic and polymer chemistries. *Science* **309,** 1200–1205 (2005).
5. Barner-Kowollik, C. *et al*. 'Clicking' polymers or just efficient linking: what is the difference? *Angew. Chem. Int. Ed.* **50,** 60–62 (2011).
6. Sletten, E. M. & Bertozzi, C. R. Bioorthogonal chemistry: fishing for selectivity in a sea of functionality. *Angew. Chem. Int. Ed.* **48,** 6974–6998 (2009).
7. Bowman, C. N. & Kloxin, C. J. Toward an enhanced understanding and implementation of photopolymerization reactions. *AIChE J.* **54,** 2775–2795 (2008).
8. DeForest, C. A., Polizzotti, B. D. & Anseth, K. S. Sequential click reactions for synthesizing and patterning three-dimensional cell microenvironments. *Nature Mater.* **8,** 659–664 (2009).
9. Luo, Y. & Shoichet, M. S. A photolabile hydrogel for guided three-dimensional cell growth and migration. *Nature Mater.* **3,** 249–253 (2004).
10. Aizawa, Y., Wylie, R. & Shoichet, M. Endothelial cell guidance in 3D patterned scaffolds. *Adv. Mater.* **22,** 4831–4835 (2010).
11. Lee, S. H., Moon, J. J. & West, J. L. Three-dimensional micropatterning of bioactive hydrogels via two-photon laser scanning photolithography for guided 3D cell migration. *Biomaterials* **29,** 2962–2968 (2008).
12. Hoffmann, J. C. & West, J. L. Three-dimensional photolithographic patterning of multiple bioactive ligands in poly(ethylene glycol) hydrogels. *Soft Matter* **6,** 5056–5063 (2010).
13. Seidlits, S. K., Schmidt, C. E. & Shear, J. B. High-resolution patterning of hydrogels in three dimensions using direct-write photofabrication for cell guidance. *Adv. Funct. Mater.* **19,** 3543–3551 (2009).
14. Kloxin, A. M., Kasko, A. M., Salinas, C. N. & Anseth, K. S. Photodegradable hydrogels for dynamic tuning of physical and chemical properties. *Science* **324,** 59–63 (2009).
15. Khetan, S., Katz, J. S. & Burdick, J. A. Sequential crosslinking to control cellular spreading in 3-dimensional hydrogels. *Soft Matter* **5,** 1601–1606 (2009).
16. Khetan, S. & Burdick, J. A. Patterning network structure to spatially control cellular remodeling and stem cell fate within 3-dimensional hydrogels. *Biomaterials* **31,** 8228–8234 (2010).
17. Sarig-Nadir, O., Livnat, N., Zajdman, R., Shoham, S. & Seliktar, D. Laser photoablation of guidance microchannels into hydrogels directs cell growth in three dimensions. *Biophys. J.* **96,** 4743–4752 (2009).
18. Ilina, O., Bakker, G. J., Vasaturo, A., Hofmann, R. M. & Friedl, P. Two-photon laser-generated microtracks in 3D collagen lattices: principles of mmp-dependent and -independent collective cancer cell invasion. *Phys. Biol.* **8,** 015010 (2011).
19. Codelli, J. A., Baskin, J. M., Agard, N. J. & Berozzi, C. R. Second-generation difluorinated cyclooctynes for copper-free click chemistry. *J. Am. Chem. Soc.* **130,** 11486–11493 (2008).
20. Adzima, B. J. *et al*. Spatial and temporal control of the alkyne-azide cycloaddition by photoinitiated Cu(II) reduction. *Nature Chem.* **3,** 258–261 (2011).
21. Hoyle, C. E. & Bowman, C. N. Thiol-ene click chemistry. *Angew. Chem. Int. Ed.* **49,** 1540–1573 (2010).
22. Dondoni, A. The emergence of thiol-ene coupling as a click process for materials and bioorganic chemistry. *Angew. Chem. Int. Ed.* **47,** 8995–8997 (2008).
23. Polizzotti, B. D., Fairbanks, B. D. & Anseth, K. S. Three-dimensional biochemical patterning of click-based composite hydrogels via thiolene photopolymerization. *Biomacromolecules* **9,** 1084–1087 (2008).
24. DeForest, C. A., Sims, E. A. & Anseth, K. S. Peptide-functionalized click hydrogels with independently tunable mechanics and chemical functionality for 3D cell culture. *Chem. Mater.* **22,** 4783–4790 (2010).
25. Killops, K. L., Campos, L. M. & Hawker, C. J. Robust, efficient, and orthogonal synthesis of dendrimers via thiol-ene 'click' chemistry. *J. Am. Chem. Soc.* **130,** 5062–5064 (2008).
26. Fairbanks, B. D. *et al*. A versatile synthetic extracellular matrix mimic via thiol-norbornene photopolymerization. *Adv. Mater.* **21,** 5005–5010 (2009).
27. Gupta, N. *et al*. A versatile approach to high-throughput microarrays using thiol-ene chemistry. *Nature Chem.* **2,** 138–145 (2010).
28. Uygun, M., Tasdelen, M. A. & Yagci, Y. Influence of type of initiation on thiol-ene 'click' chemistry. *Macromol. Chem. Phys.* **211,** 103–110 (2010).
29. Alvarez, M. *et al*. Single-photon and two-photon induced photocleavage for monolayers of an alkyltriethoxysilane with a photoprotected carboxylic ester. *Adv. Mater.* **20,** 4563–4567 (2008).
30. Deiters, A. Principles and applications of the photochemical control of cellular processes. *ChemBioChem* **11,** 47–53 (2010).
31. Holmes, C. P. Model studies for new *o*-nitrobenzyl photolabile linkers: substituent effects on the rates of photochemical cleavage. *J. Org. Chem.* **62,** 2370–2380 (1997).
32. Ohmuro-Matsuyama, Y. & Tatsu, Y. Photocontrolled cell adhesion on a surface functionalized with a caged arginine-glycine-aspartate peptide. *Angew. Chem. Int. Ed.* **47,** 7527–7529 (2008).
33. Johnson, J. A., Baskin, J. M., Bertozzi, C. R., Koberstein, J. T. & Turro, N. J. Copper-free click chemistry for the *in situ* crosslinking of photodegradable star polymers. *Chem. Commun.* 3064–3066 (2008).
34. Wong, D. Y., Griffin, D. R., Reed, J. & Kasko, A. M. Photodegradable hydrogels to generate positive and negative features over multiple length scales. *Macromolecules* **43,** 2824–2831 (2010).
35. Kloxin, A. M., Tibbitt, M. W. & Anseth, K. S. Synthesis of photodegradable hydrogels as dynamically tunable cell culture platforms. *Nature Protoc.* **5,** 1867–1887 (2010).
36. Kloxin, A. M., Benton, J. A. & Anseth, K. S. *In situ* elasticity modulation with dynamic substrates to direct cell phenotype. *Biomaterials* **31,** 1–8 (2010).
37. Frey, M. T. & Wang, Y. L. A photo-modulatable material for probing cellular responses to substrate rigidity. *Soft Matter* **5,** 1918–1924 (2009).
38. Redick, S. D., Settles, D. L., Briscoe, G. & Erickson, H. P. Defining fibronectin's cell adhesion synergy site by site-directed mutagenesis. *J. Cell Biol.* **149,** 521–527 (2000).
39. Sims, E. A., DeForest, C. A. & Anseth, K. S. A mild, large-scale synthesis of 1,3-cyclooctanedione: expanding access to difluorinated cyclooctyne for copper-free click chemistry. *Tetrahedron Lett.* **52,** 1871–1873 (2011).

Acknowledgements

The authors thank A. Kloxin and M. Tibbitt for useful discussions regarding photopatterning, C-C. Lin for advice on cell outgrowth experiments, A. Aimetti and P. Hume for communication on general experimental design, and C. Kloxin for insightful feedback on the written manuscript. Fellowship assistance to C.A.D. was awarded by the US Department of Education's Graduate Assistantships in Areas of National Need. This work was made possible by financial support from the National Science Foundation (DMR 1006711) and the Howard Hughes Medical Institute.

Author contributions

C.A.D. and K.S.A. developed the material concept. C.A.D. and K.S.A. designed the experiments. C.A.D. carried out the experiments. C.A.D. and K.S.A. wrote the manuscript.

Additional information

The authors declare no competing financial interests. Supplementary information accompanies this paper at www.nature.com/naturechemistry. Reprints and permission information is available online at http://www.nature.com/reprints. Correspondence and requests for materials should be addressed to K.S.A.